

**SIMULATION OF STRUCTURES AND  
POWDER DIFFRACTION PATTERNS  
OF  $\alpha$ -Ga<sub>2</sub>O<sub>3</sub> AND  $\beta$ -Ga<sub>2</sub>O<sub>3</sub>**



**FIZZA AFTAB**

**DEPARTMENT OF PHYSICS  
KINNAIRD COLLEGE FOR WOMEN,  
LAHORE, PAKISTAN  
2023**

**SIMULATION OF STRUCTURES AND  
POWDER DIFFRACTION PATTERNS  
OF  $\alpha$ -Ga<sub>2</sub>O<sub>3</sub> AND  $\beta$ -Ga<sub>2</sub>O<sub>3</sub>**



**A RESEARCH REPORT SUBMITTED TO  
KINNAIRD COLLEGE FOR WOMEN  
IN FULFILMENT OF THE REQUIREMENTS  
FOR THE DEGREE OF  
BACHELORS OF SCIENCE  
IN  
PHYSICS**

**BY**

**FIZZA AFTAB**

**DEPARTMENT OF PHYSICS**

**KINNAIRD COLLEGE FOR WOMEN, LAHORE**

**2023**

## RESEARCH COMPLETION CERTIFICATE

It is certified that **Ms. Fizza Aftab** of BS (session 2019-2023), Department of Physics has carried out research work entitled “**Simulation of Structures and Powder Diffraction Patterns of  $\alpha$ -Ga<sub>2</sub>O<sub>3</sub> and  $\beta$ -Ga<sub>2</sub>O<sub>3</sub>**” under my supervision.

It is assured that research work is original and has not yet been published anywhere else.

**Supervisor:**

Dated: 17-05-2023

\_\_\_\_\_  
**Ayesha Aftab**

Head of Physics Department

Kinnaird College for Women, Lahore.

\_\_\_\_\_  
**Ayesha Aftab**

Head of Physics Department

Kinnaird College for Women, Lahore.

“All changes suggested by examiners during defense are incorporated in this final copy.”

\_\_\_\_\_  
Student

\_\_\_\_\_  
Supervisor

\_\_\_\_\_  
Head of Department

## ANTI-PLAGIARISM DECLARATION

I certify that this is my own research work. The work has not, in whole or in part, been presented elsewhere for assessment. Where material has been used from other sources, it has been properly acknowledged. The similarity index of the research report is 14%. If this statement is untrue and I am found guilty of plagiarism, the punitive action against me should be taken as per Kinnaird Anti Plagiarism Policy.

**Fizza Aftab**

Registration No: F19BPHY002

Program: BS PHYSICS

Signature:

**Supervisor:**

---

**Aysha Aftab**

Head of Physics Department

Kinnaird College for Women, Lahore.

---

**Aysha Aftab**

Head of Physics Department

Kinnaird College for Women, Lahore.

## **ACKNOWLEDGEMENTS**

I will be eternally grateful to Kinnaird College for Women for not only providing a progressive environment with comprehensive knowledge but also the encouragement for being confident and skillful in life and motivation to become a better person. It is a great pleasure to acknowledge and express my deepest thanks and gratitude to my supervisor Ma'am Aysha Aftab for her constant guidance, cooperation, continuous motivation and immense knowledge. Her instructions have helped me a lot throughout the research work to overcome various challenges and limitations. I would also like to thank my senior Zainab Nasir for her immense guidance and assistance in my research work which really helped me a lot. I'd want to thank my all teachers, family and friends who assisted, supervised, accompanied and motivated with supportive hugs in moments of stress. Worthy of special mention is my father who stood by me since day one. I am much thankful for his unwavering support and contribution to my academic success.

**Fizza Aftab**

## ABSTRACT

Silicon is approaching the peak of its performance, and basic limitations on its materials properties. A new oxide semiconducting material gallium oxide is a perfect material for the power devices in very high voltage applications.  $\text{Ga}_2\text{O}_3$  has several crystalline forms, such as  $\alpha$ ,  $\beta$ ,  $\gamma$  and  $\delta$  phases, with different properties and applications. For example, the  $\beta$ - $\text{Ga}_2\text{O}_3$  phase has a wider band gap compared to  $\alpha$  phase and is suitable for UV optoelectronic devices. Fabrication and characterization of  $\text{Ga}_2\text{O}_3$  based devices have been ongoing for several years, with recent breakthroughs in the growth of high-quality single-crystal substrates and development of high-performance devices. Superior material properties of Gallium Oxide, especially a significantly larger band gap than those of Silicon Carbide and Gallium Nitride, aptitude power devices with higher  $V_{br}$  and efficiency than Silicon Carbide and Gallium Nitride counterparts. Another significant feature of  $\text{Ga}_2\text{O}_3$  is that instinctive substrates can be created from bulk single crystals grown using the same melt-growth procedures as sapphire substrates. In this research work, two of five polymorphs of Gallium Oxide are theoretically analyzed. From literature review, it was observed that the  $\beta$  phase exists as most stable polymorph. VESTA Software was used to achieve better understanding of different parameters in terms of crystal structures, XRD patterns, fractional coordinates and lattice planes for  $\text{Ga}_2\text{O}_3$   $\alpha$  and  $\beta$  polymorphs. Challenges remain in the processing and scaling up of  $\text{Ga}_2\text{O}_3$ -based devices, as well as improving their efficiency and reliability. Overall,  $\text{Ga}_2\text{O}_3$ , is a favorable material for advanced power electronics, optoelectronics and sensing applications, and ongoing research is expected to lead to new breakthroughs and commercialization of  $\text{Ga}_2\text{O}_3$ -based devices soon.

# SIMULATION OF STRUCTURES AND POWDER DIFFRACTION PATTERNS OF $\alpha$ -Ga<sub>2</sub>O<sub>3</sub> AND $\beta$ -Ga<sub>2</sub>O<sub>3</sub>

## TABLE OF CONTENTS

Chapter	Title	Page
	<b>RESEARCH COMPLETION CERTIFICATE.....</b>	ii
	<b>ANTI-PLAGIARISM DECLARATION.....</b>	iii
	<b>ACKNOWLEDGEMENTS.....</b>	iv
	<b>ABSTRACT.....</b>	v
	<b>TABLE OF CONTENTS.....</b>	vi
	<b>LIST OF FIGURES.....</b>	x
	<b>LIST OF TABLES.....</b>	xi
	<b>ABBREVIATIONS.....</b>	xii
<b>1</b>	<b>INTRODUCTION.....</b>	<b>1</b>
	1.1 Crystalline Solids.....	1
	1.2 Crystal Structure.....	1
	1.3 Lattice Translational Vectors.....	1
	1.4 Unit Cell.....	2
	1.5 Lattice System.....	2
	1.5.1 Bravais Lattice.....	3
	1.5.2 Miller Indices.....	3
	1.5.3 Description of Crystal Structure.....	3
	1.6 Transparent Conducting Oxide.....	4
	1.7 Presence of Elements in Periodic Table.....	4
	1.8 Gallium.....	4
	1.8.1 Gallium Oxide.....	5
	1.8.2 Widespread Adoption of Gallium Oxide.....	5

1.9 Polymorphs of Gallium Oxide.....	6
1.10 Computational Modeling.....	9
1.10.1 Modeling of Crystal Structure.....	9
1.10.2 Types of Crystal Modeling.....	9
1.10.3 Isometric or Cubic.....	10
1.10.4 Tetragonal.....	10
1.10.5 Orthorhombic.....	10
1.10.6 Monoclinic.....	10
1.10.7 Triclinic.....	10
1.10.8 Hexagonal.....	10
1.11 Classifications of Solids.....	11
1.11.1 Crystalline Solids.....	11
1.11.2 Motion of Atoms, Ions and Molecules.....	11
1.11.3 Amorphous or Glassy Solids.....	11
1.11.4 Polymeric Solids.....	11
1.12 XRD.....	11
1.12.1 Plot of Intensity.....	12
1.12.2 Applications of Powder Diffraction Pattern.....	13
1.13 Applications for Analyzing Crystal Structures.....	13
<b>RATIONALE.....</b>	<b>14</b>
<b>OBJECTIVES.....</b>	<b>15</b>
<b>2 LITERATURE REVIEW.....</b>	<b>16</b>
<b>3 METHODOLOGY.....</b>	<b>21</b>
3.1 Visualization of Electronic and Structural Analysis.....	21
3.1.1 Introduction.....	21
3.1.2 Features of VESTA.....	21
3.1.3 Visualization of Structural Models.....	22
3.2 Display Crystallographic Information.....	22
3.3 Lattice Transformation.....	22
3.4 Dealing with Volumetric Data.....	22

3.4.1 Visualization of Volumetric Data.....	22
3.4.2 Pixel Operation of Multiple 3D Data.....	23
3.4.3 Surface Coloring.....	23
3.4.4 Display Lattice Planes and Crystal Morphologies.....	24
3.5 Construction of Structure of $\alpha$ -Ga <sub>2</sub> O <sub>3</sub> .....	24
3.5.1 Main window.....	24
3.5.2 Unit Cell.....	24
3.5.3 Selection of Parameters.....	25
3.6 Construction of Structure of $\beta$ -Ga <sub>2</sub> O <sub>3</sub> .....	25
3.6.1 Main Window.....	25
3.6.2 Unit Cell.....	25
3.6.3 Selecting Parameters.....	25
3.7 Crystal Structure Models.....	26
3.7.1 Ball and Stick.....	26
3.7.2 Space Filling.....	26
3.7.3 Polyhedral.....	26
3.7.4 Wireframe.....	27
3.7.5 Stick.....	27
3.8 Lattice Planes.....	27
3.8.1 Interplanar Distances.....	27
3.8.2 Lattice Planes Insertion in $\alpha$ -Ga <sub>2</sub> O <sub>3</sub> Unit Cell.....	28
3.8.3 Lattice Planes Insertion in $\beta$ -Ga <sub>2</sub> O <sub>3</sub> Unit Cell.....	28
3.9 Ranges of Fractional Coordinates.....	28
3.9.1 In case of $\alpha$ -Ga <sub>2</sub> O <sub>3</sub> .....	28
3.9.2 In case of $\beta$ -Ga <sub>2</sub> O <sub>3</sub> .....	28
3.10 Powder Diffraction Patterns.....	28
<b>4 RESULTS AND DISCUSSION.....</b>	<b>29</b>
4.1 Crystallographic Models for $\alpha$ -Ga <sub>2</sub> O <sub>3</sub> .....	29
4.2 Crystallographic Models for $\beta$ -Ga <sub>2</sub> O <sub>3</sub> .....	30
4.3 Ranges of Fractional Coordinates for $\alpha$ -Ga <sub>2</sub> O <sub>3</sub> .....	31

4.4 Ranges of Fractional Coordinates for $\beta$ -Ga <sub>2</sub> O <sub>3</sub> .....	32
4.5 Lattice Planes for $\alpha$ -Ga <sub>2</sub> O <sub>3</sub> .....	32
4.6 Lattice Planes for $\beta$ -Ga <sub>2</sub> O <sub>3</sub> .....	33
4.7 Powder Diffraction Pattern for $\alpha$ -Ga <sub>2</sub> O <sub>3</sub> .....	34
4.8 Powder Diffraction Pattern for $\beta$ -Ga <sub>2</sub> O <sub>3</sub> .....	34
<b>CONCLUSION</b> .....	<b>37</b>
<b>LIMITATIONS</b> .....	<b>38</b>
<b>REFERENCES</b> .....	<b>39</b>

## LIST OF FIGURES

Figures	Title	Page
1.1	Primitive Unit Cell.....	2
1.2	Planes with varying Miller Indices.....	3
1.3	$\alpha$ -Ga <sub>2</sub> O <sub>3</sub> Structure.....	7
1.4	$\beta$ -Ga <sub>2</sub> O <sub>3</sub> Structure.....	8
1.5	$\gamma$ -Ga <sub>2</sub> O <sub>3</sub> Structure .....	8
1.6	$\epsilon$ and $\delta$ -Ga <sub>2</sub> O <sub>3</sub> Structure .....	9
1.7	Seven Crystal Systems.....	10
1.8	Diffractionmeter's Equipment.....	12
3.1	Main Window.....	24
3.2	Selecting Structural Parameters of $\alpha$ -Ga <sub>2</sub> O <sub>3</sub> .....	25
3.3	Structural Parameters for $\beta$ -Ga <sub>2</sub> O <sub>3</sub> .....	26
3.4	Inserting Lattice Planes.....	28
4.1	$\alpha$ -Ga <sub>2</sub> O <sub>3</sub> Crystallographic Models.....	29
4.2	$\beta$ -Ga <sub>2</sub> O <sub>3</sub> Crystallographic Models .....	30
4.3	Ranges of Fractional Coordinates in $\alpha$ -Ga <sub>2</sub> O <sub>3</sub> .....	31
4.4	Ranges of Fractional Coordinates in $\beta$ -Ga <sub>2</sub> O <sub>3</sub> .....	32
4.5	Lattice Planes in $\alpha$ -Ga <sub>2</sub> O <sub>3</sub> .....	33
4.6	Lattice Planes in $\beta$ -Ga <sub>2</sub> O <sub>3</sub> .....	33
4.7	XRD Patterns for $\alpha$ -Ga <sub>2</sub> O <sub>3</sub> .....	34
4.8	XRD Patterns for $\beta$ -Ga <sub>2</sub> O <sub>3</sub> .....	35

## LIST OF TABLES

Table	Title	Page
1.1	Semiconductor Material Properties.....	5
1.2	Structural Parameters of Ga <sub>2</sub> O <sub>3</sub> polymorphs.....	7
4.1	Lattice Parameters and Atomic Positions for $\alpha$ -Ga <sub>2</sub> O <sub>3</sub> .....	36
4.2	Lattice Parameters and Atomic Positions for $\beta$ -Ga <sub>2</sub> O <sub>3</sub> .....	36

## ABBREVIATIONS

3D	Three Dimensional
Bcc	body-centered cubic
Fcc	face-centered cubic
TCO	Transparent Conducting Oxide
Ccp	cubic closed packed
Hcp	hexagonal closed packed
XRD	X-ray diffraction
$\Theta$	Angle
$\Lambda$	Wavelength
VESTA	Visualization for Electronic and Structural Analysis
$D_{hkl}$	spacing $d$ between adjacent (h k l)
UV	Ultraviolet
IR	Infrared Rays

# CHAPTER 1

## INTRODUCTION

### 1.1 Crystalline Solids

Solid molecules do not move, they merely vibrate and spin in place. These are held together by either ionic or a covalent bonding, provided that the attractive forces between the atoms, ions, or molecules in solids are sturdy. Forces are so robust that the solid particles are kept in settled places with minimum flexibility of motion. Solid materials have distinct forms and volumes, and they are not compressible [1].

Solids are classified into two types: crystalline solids and amorphous solids. Crystalline solids have atoms or molecules that are arranged in a regular, well-defined manner. Amorphous solids are the other primary form of solid. The structures of amorphous solids are disordered. Despite the fact that their molecules are densely packed and have little freedom of movement, they are not ordered in a regular sequence as in crystalline materials [1].

### 1.2 Crystal Structure

A perfect crystal is made by infinitely repeating identical groups of atoms. A basis is an accumulation of atoms. A set of the mathematical points on which the basis is connected is called Lattice. The structure of a crystal is generated by adding basis to each space lattice point [1,3].

It is composed of either one or more than one-unit cells which are described as the fewest atoms required to define an entire crystal structure. This is likely to happen as the structure is periodic, i.e., it repeats. This arrangement is known as a crystal lattice. The number of atoms in the basis could be one or more than one. Every basis in each crystal is the same in composition, organization, and alignment [1].

### 1.3 Lattice Translational Vectors

The three-dimensional lattice can be well-defined by the three translational vectors  $\mathbf{a}_1$ ,  $\mathbf{a}_2$ ,  $\mathbf{a}_3$ , so that the arrangement of atoms in the crystal looks the same when viewed from the point  $\mathbf{r}$  as when viewed from every point  $\mathbf{r}'$  that is translated by an integral multiple of  $\mathbf{a}$ 's:

$$\mathbf{r}' = \mathbf{r} + u_1\mathbf{a}_1 + u_2\mathbf{a}_2 + u_3\mathbf{a}_3$$

Here  $u_1, u_2, u_3$  are arbitrary integrals. The points *set*  $\mathbf{r}'$  that are well-defined by the above equation for all  $u_1, u_2, u_3$  describes the lattice [3].

### 1.4 Unit Cell

A crystal's structure can be observed to be formed of a recurring constituent in three dimensions. The unit cell is an essential component of crystal forms, distinguished by its lattice points. Non-primitive unit cells feature several lattice points, whereas primitive unit cells have only one. The unit cell used is decided by the crystal structure and the desired level of information [3].

Primitive cells are preferred in certain cases, such as when calculating physical properties or studying defects in the crystal. Primitive unit cells have the smallest volume and the simplest lattice structure, making them useful for determining crystal symmetry and calculating physical properties. The choice of unit cell depends on the crystal structure and the desired level of detail. For example, in the face-centered cubic lattice, a primitive unit cell consists of one-eighth of each corner atom and one-half of each face-centered atom. However, a non-primitive unit cell can be constructed that contains all of the corner atoms and face-centered atoms. Unit cells are classified into two types: primitive and non-primitive [3].

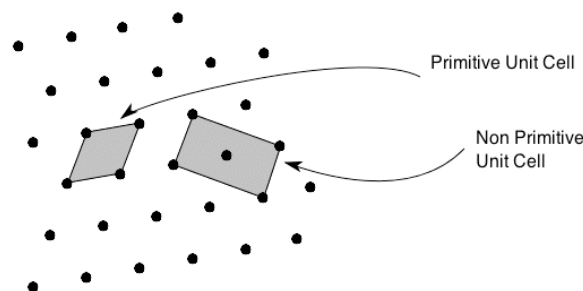


Figure 1.1 Primitive Unit Cell [3]

## 1.5 Lattice System

To characterize their lattice, lattice systems are described as a collection of crystal structures categorized according to the axial system. Every lattice system has a set with three axes in a certain geometric configuration. The cubic or isometric lattice system is the most basic and symmetric lattice system. There are six other lattice systems: hexagonal, triclinic, tetragonal, orthorhombic, and monoclinic [4].

### 1.5.1 Bravais Lattice

Bravais lattices are lattice point geometric configurations having structural translational symmetry. There are fourteen distinct Bravais lattices in three dimensions of space, which explains translational symmetries. The Bravais lattice is regarded to be the basic core component from which all crystals are built. These lattices are comprised in seven distinct crystal systems characterized by the relationship between unit cell angles, sides, and distance between unit cell points [4,5].

### 1.5.2 Miller Indices

The three-value Miller index system can be used to describe axes and planes in a lattice structure. The indices  $l$ ,  $m$ , and  $n$  are used in the syntax for directional parameters. This syntax  $(l\ m\ n)$  represents a plane. Miller indices are generally equal to the inverse of plane intercepts, with the unit cell serving as the origin of the lattice vector. If one or more of the indices is 0, the planes will not intersect that axis. A negative index is indicated by a horizontal bar on the numerals [4].

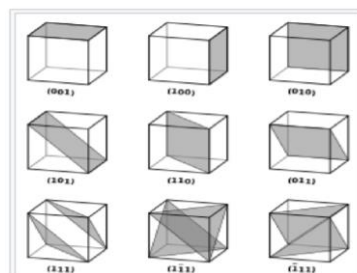


Figure 1.2 Planes with different Miller Indices [4]

### 1.5.3 Description of Crystal Structure

There are various ways to describe crystal forms. The most frequent method is to identify the unit cell's size and shape, as well as the positions of the atoms or ions within the cell.

This level of comprehension is frequently insufficient for comprehending three-dimensional structures. To have a better knowledge of a crystal structure, multiple unit cells must be examined, as well as the arrangement of atoms, ions, and molecules in relation to one another, the number of other atoms in contact with atoms, and the distance between atoms. There are several approaches of describing extended solid-state systems [5].

### **1.6 Transparent Oxide Semiconductors**

The transparent oxides that are conductive are a rare substance. They are translucent in the visible spectrum, with a transmittance of more than 80%, and conductive in the infrared spectrum, with a resistivity of less than  $10^3$  cm, allowing them to be employed in a variety of technical devices such as solar cells, display panels, and thin-film transparent field effect transistors. Oxides generated by the combination of two or more binary oxides, such as  $\text{In}_2\text{O}_3$ ,  $\text{Ga}_2\text{O}_3$  and Zinc Oxide have been examined to increase the quality of material. Such multiterinary combinations can be either amorphous or crystalline [6].

LEDs, photovoltaic cells, contact panels, and translucent tinny film transistors are all examples of TCOS uses. Balanced and regular pairings of n-type and p-type transparent semiconductors are required for the ultimate transparent electronic devices. Whereas numerous transparent oxide semiconductors of n type, such as Indium Gallium Zinc Oxide and ZnO, are commercially accessible and utilized in electronics, there are basically no p-type oxides that are comparable to their n-type counterparts, despite significant efforts to find them. Recently, high-throughput screening was used to find probable p-type transparent oxides using DFT calculations; nevertheless, none of reported semiconductor were empirically validated, emphasizing the need for a more effective theoretical predictor [7].

### **1.7 Presence of Elements in Periodic Table**

The periodic table is regarded as a tabular representation of elements. The periodic table is divided into four rectangular areas called blocks that are s, p, d, and f blocks. In periodic table rows are considered as periods while the columns in table are known as groups. Elements associated with the same column group exhibit similar chemical characteristics. In a table, the trend goes through with non-metallic character increasing throughout a period, it moves from left to right and across a group it moves from down to up. Metallic

nature will increase in the opposite direction. There are 118 elements known out of which first ninety-four elements occur in nature and other elements are artificially created [8].

## **1.8 Gallium**

Gallium is a periodic table chemical element having the atomic number 31 and the represented as Ga. It belongs to the Boron family (group 13) and is in period 4.

Gallium is a solid bluish grey metal. Holding a lump of gallium in your palm will cause it to liquefy since gallium melts at temperatures higher than room temperature. Gallium is a soft metal that can be easily sliced with a knife. It is stable in air and water, but dissolves when exposed to acids and alkalis. Gallium expands by 3.1 percent while hardening, making it unsuitable for storage in glass or metal [9].

### **1.8.1 Gallium Oxide**

In the 1960s, scientists began researching the different configurations of gallium oxide. The emphasis switched in the year 2000 to structural studies of gallium oxide using the arc discharge method. Many groups used the arc discharge method to create monoclinic  $\text{Ga}_2\text{O}_3$  nanowires. Silicon is looming the highpoint of its performance, and inherent material restrictions rule out several applications. For instance, an indirect band gap energy of 1.1 eV results in low light absorption and radiative recombination efficiency, restricting its use in optoelectronics [9].

$\text{Ga}_2\text{O}_3$  belongs to a family of conducting transparent semiconducting oxides (TSO) [31]. Its band gaps are much wider than those of Silicon Carbide with bandgap 3.3 eV and Gallium Nitride (3.4 eV), which forms gallium oxide an appealing TCO for forthcoming power electronic applications, like UV photodetectors. The monoclinic phase is its most balanced form, with a high band gap, strong conductivity and breakdown field, and good transparency in the UV spectral range [7,30].

Table 1.1 Semiconductor Material Properties [15]

	Si	SiC	GaN	$\beta$ -Ga <sub>2</sub> O <sub>3</sub>
Bandgap (eV)	1.12	3.26	3.4	4.9
Dielectric constant $\epsilon$	11.9	9.7	9.5	10
Electron mobility $\mu$ (cm <sup>2</sup> /Vs)	1350	1000	900	300(est.)
Thermal conductivity (W/cmK)	1.5	4.9	2	0.14
Breakdown voltage $E_b$ (MV/cm)	0.3	2.7	3.5	8(est.)
BFOM <sup>†</sup> (cmE <sub>b</sub> <sup>3</sup> )	1	340	870	3444

### 1.8.2 Widespread Adoption of Gallium Oxide

Global efforts to assure reliable energy provisions in the near future have increased demand for innovative energy sources to substitute fossil fuels, as well as concepts for cutting-edge skills to realize competent energy generation and utilization. Gallium Oxide has a higher critical field strength and thermal conductivity than Silicon Carbide and Gallium Nitride, making it a promising candidate for ultrahigh voltage switching applications requiring high power density and thermal control. Gallium Oxide's unique features enable the creation of power devices with much higher operating temperatures and greater tolerance to common mode voltage strains. Its wider band-gap also allows for improved current flow insulation, resulting in lower power loss and higher efficiency. Gallium Oxide is thus a promising material for use in ultrahigh voltage switching applications where power efficiency and reliability are critical. The superior material properties of Gallium Oxide have demonstrated its potential to surpass the performance of more commonly used semiconductors such as Silicon Carbide and Gallium Nitride in high-power electronic devices [13].

Native substrates of Gallium Oxide can be produced on a mass scale, providing a cost-effective solution for the production of Gallium Oxide-based structures, making it possible to grow bulk single crystals of Gallium Oxide using the same methods used to grow sapphire. These procedures involve melting the raw material and then allowing it to slowly cool, allowing the crystals to form. This means that Gallium Oxide substrates can be synthesized on a large scale without requiring new and expensive equipment or techniques. Traditional methods for growing Gallium Oxide substrates, such as chemical vapor deposition, are not well established and are still under development. This makes the melt-

growth procedures used for sapphire an attractive option for producing large, high-quality, cost-effective substrates for Gallium Oxide-based electronic devices [11].

Gallium Oxide's ability to be synthesized using established melt-growth techniques used to produce sapphire substrates makes it an appealing option for large-scale commercial production. This provides a promising path towards the widespread adoption of Gallium Oxide in high-power electronic devices, given that suitable substrates are necessary for the fabrication of electronic devices [10].

### 1.9 Polymorphs of Ga<sub>2</sub>O<sub>3</sub>

Polymorphism is derived from a Greek term. It depends on mostly two terms “Polus” and “Morph”. “Polus” means “many” while on other hand the term “morph” represents “shapes”. Polymorphism is an abbreviation meaning "many shapes." Polymorphism refers to a solid material's capacity to exist in much more than one state, whether it be in crystal structure or even in phases, and to have varied configurations and conformations of atoms in the crystalline lattice. Polymorphs are substances who have the same composition but a distinctive crystal structure [17].

Table 1.2 Structural parameters of Ga<sub>2</sub>O<sub>3</sub> Polymorphs [4]

Polymorph of Ga <sub>2</sub> O <sub>3</sub>	Structure	Space group	Lattice parameters
$\alpha$	Rhombohedral	R-3 c	$a = 4.9825 \text{ \AA}$ , $c = 13.433 \text{ \AA}$
$\beta$	Monoclinic	C2/m	$a = 12.23 \text{ \AA}$ , $b = 3.04 \text{ \AA}$ , $c = 5.80 \text{ \AA}$
$\gamma$	Cubic	Fd-3 m	$a = b = c = 8.45 \text{ \AA}$
$\delta$	Body-centered cube	La3	$a = 9.401$
$\epsilon$	Orthorhombic	Pna21	$a = 5.046 \text{ \AA}$ , $b = 8.634 \text{ \AA}$ , $c = 9.209 \text{ \AA}$

- **$\alpha$ -Ga<sub>2</sub>O<sub>3</sub>**

Corundum-Ga<sub>2</sub>O<sub>3</sub> is a member of the trigonal R-3c space group ( $a = 5.05952$ ,  $c = 13.62480$ ,  $\alpha = \beta = \gamma = 90$ ). Six analogous O (1) atoms are joined to form a mixture of deformed edge, face, and corner-sharing GaO<sub>6</sub> octahedra [11].

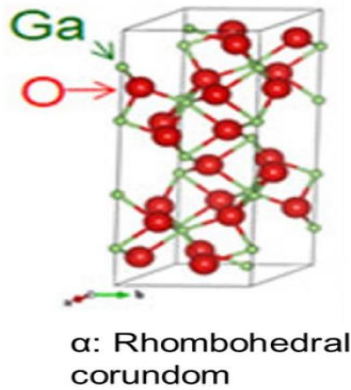


Figure 1.3  $\alpha$ - $\text{Ga}_2\text{O}_3$  Structure [11]

- **$\beta$ - $\text{Ga}_2\text{O}_3$**

A  $C2/m$  space group exists in the monoclinic structure of  $\text{Ga}_2\text{O}_3$  ( $a = 12.45245$ ,  $b = 3.08297$ ,  $c = 5.87615$ ,  $\alpha = \gamma = 90$ ,  $\beta = 103.68360$ ). There is two unique Ga- sites in  $\text{Ga}_2\text{O}_3$ , Ga (1) and Ga (2), as well as three distinct O- sites, O (1), O (2), and O (3). Ga (1) atoms are connected to two equivalent O (1), O (2), and O (3) to form a tetrahedral structure. Ga (2) atoms are bonded to one O (1), three equivalent O (2), and two equivalent O (3) atoms to construct an octahedral arrangement [11, 12].

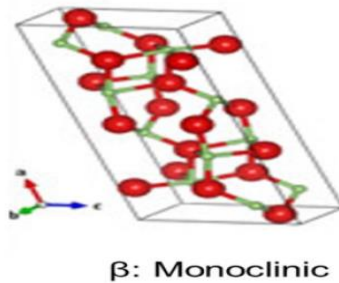


Figure 1.4  $\beta$ - $\text{Ga}_2\text{O}_3$  Structure [11]

- **$\epsilon$ - $\text{Ga}_2\text{O}_3$**

Orthorhombic  $\epsilon$ - $\text{Ga}_2\text{O}_3$  (also known as  $\kappa$  -phase) crystallizes in orthorhombic system  $CmCm$  space group ( $a = 2.82039$ ,  $b = 9.39439$ ,  $c = 7.28403$ ,  $\alpha = \beta = \gamma = 90$ ). The structure has two incompatible Ga- sites, Ga (1) and Ga (2), as well as two incompatible O sites, O (1) and O (2). Four O (1) and two O (2) atoms near together form bonds with Ga (1). Bonding four O (1) and two O (3) atoms results in a mixture of edge and corner-sharing  $\text{GaO}_6$  octahedra [11].

- $\gamma\text{-Ga}_2\text{O}_3$

$\gamma\text{-Ga}_2\text{O}_3$  has defective cubic spinel-type structure ( $\text{MgAl}_2\text{O}_3$ -type) with  $\text{Fd}3\text{m}$  space group [11].

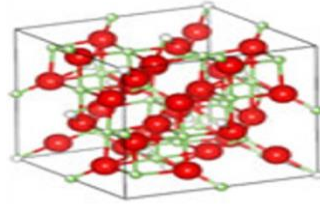


Figure 1.5 shows  $\gamma$ - Phase [11]

- $\delta\text{-Ga}_2\text{O}_3$

The fifth polymorphs, called  $\delta\text{-Ga}_2\text{O}_3$  was first synthesized and described in 1952. The authors proposed that  $\delta\text{-Ga}_2\text{O}_3$  form has a C-type rare-earth structure [11].

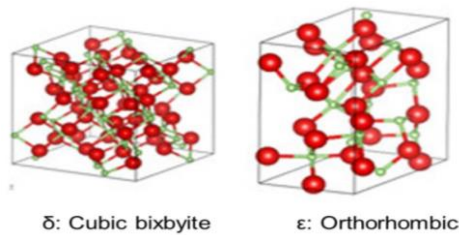


Figure 1.6 shows  $\epsilon$  and  $\delta\text{-Ga}_2\text{O}_3$  structures [11]

## 1.10 Computational Modeling

Crystallography is the discipline of study concerned with the organization and bonding of atoms found in crystalline materials, as well as the geometric structure of accessible crystalline lattice. Crystal optical characteristics are helpful in mineralogy and sciences for identifying compounds. It is important to find out the arrangement of atoms in materials to identify the relationship between their properties and atomic structures [28,29].

### 1.10.1 Modeling of Crystal Structure

When developing or creating experimental settings seems to be either impossible or difficult, modelling is utilized to replace direct measurement and experimentation. Modeling theorems is indeed a scientific activity. By altering parameters, it is feasible to perform a specific aspect or the whole behavior of experimental data that is more accessible

or simpler to comprehend, visualize, characterize, and reproduce. Graphical models are often utilized to visualize the various material properties [17].

### 1.10.2 Types of Crystals Modeling

The following six crystal systems are important for modeling atoms and molecules [18].

- Isometric or cubic
- Tetragonal
- Orthorhombic
- Monoclinic
- Triclinic
- Hexagonal

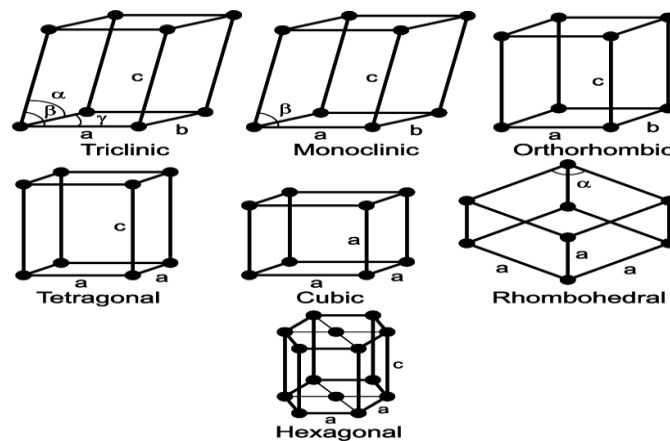


Figure 1. 7 Seven Crystal Systems [14]

### 1.10.3 Isometric or Cubic

This system is composed of crystal containing three axes, which are all perpendicular to each other have identical lengths [18].

### 1.10.4 Tetragonal

This system is made up of crystal having three axes, which are all perpendicular to each other, just two of which are similar in length [18].

### 1.10.5 Orthorhombic

This system is made up of crystal featuring three mutually perpendicular axes, each of which has a distinct length [18].

### 1.10.6 Monoclinic

This system is made up of crystal bearing three axes that are all uneven in length. Two of the axes really are not perpendicular to one another, however they are perpendicular to the third [18].

#### **1.10.7 Triclinic**

This system is made up of crystal comprising three axes, all of which are uneven in length and are therefore not perpendicular to each other [18].

#### **1.10.8 Hexagonal**

This system is made up of four-axed crystals. Three of among these axes seem to be in a single plane, are properly spaced, and are of equal lengths. The fourth axes are perpendicular to all three axes [18].

### **1.11 Classification of Solids**

In concern with study of structure and properties, solids are classified as:

- Crystalline Solids
- Amorphous Solids or glassy Solids
- Polymeric Solids

#### **1.11.1 Crystalline Solids**

Crystalline solids are ones in which the atoms and molecules are arranged in a regular pattern. Every molecule's neighbor is organized in a predictable manner that is consistent all across the crystal. The ordered structure of crystalline solids can be studied by x-rays diffraction techniques. Some examples of crystalline solids are copper, iron, zinc, zirconia, and silicon etc. [19].

#### **1.11.2 Motion of atoms, ions, and molecules**

Atoms, ions, and molecules in a crystalline solid are in state of vibratory motion about fixed points. Their amplitude of vibration increases with the increase in temperature. But the average distance between the atomic positions remains the same [19].

#### **1.11.3 Amorphous or Glassy Solids**

There is no predictable distribution of atoms in amorphous solids, they are much like fluids with chaotic structures frozen in them. They are called solid liquids. They have no definite melting point [19].

#### 1.11.4 Polymeric Solids

They are solid materials having a structure that lies somewhere between order and conflict. Polymerization relates to the procedure by which comparatively simple molecules are joined into huge, long chains or three-dimensional structures via chemical processes [19].

### 1.12 XRD

It is a process used in research of substances to verify material's crystalline structure. XRD involves exposing any material to arriving X-rays and thereafter evaluating the intensity as well as spreading angles of such X-rays that depart the material [24].

To define and determine the lattice parameters of a crystal structure diffraction patterns are used. Whenever the X-ray is directed at a crystal, it causes it to diffract in way exceptional to structure. The diffraction peaks are derived from any material powder rather than a single crystal. It is simpler, more effective, and economical than a single crystal diffraction as creation of individual crystals is not needed [21].

#### 1.12.1 Plot of Intensity

An XRD pattern is a graph of the intensity of the X-rays distributed at different angles obtained with a specimen consisting of an X-ray source (often an X-ray tube), detector, angle-changing mechanism, and sample container. To begin, an X-ray is directed at an angle on the material, and the detector is placed in the opposite direction of the source, detecting the intensity of the X-ray received at an angle of  $2\theta$  from the source route. The detector angle is constantly  $2\theta$  above the source path, whereas the incidence angle grows progressively.

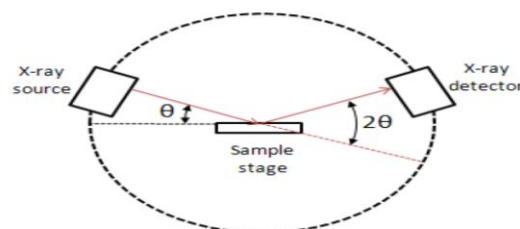


Figure 1.8 Diffractometer's equipment [21]

$$\sin\theta = n\lambda/2d$$

$\theta$  is the angle of the incidence of the X-ray,  $n$  is an integer,  $\lambda$  is the wavelength whereas  $d$  is the spacing between atom layers. As a result, constructive interference as well as a peak in intensity will occur. This X-ray signal is recorded and processed by a detector, which then transforms the signal to an intensity ratio that is sent to a machine [21,22].

### **1.12.2 Applications of Powder X-ray Diffraction**

The most common use of X-ray powder diffraction is to identify an unknown crystalline substance. The following are some applications of powder X-ray diffraction.

- Crystalline material characteristics
- Identifying fine-grained minerals
- Calculating unit cell dimensions
- Determine crystal structures [22].

### **1.13 Applications for analyzing Crystal Structures**

Analyzing crystal structure on the basis of x-ray crystallography will give hundreds of applications. It was mostly employed in basic scientific applications. To determine the size of atoms, the molecular geometry of materials, the lengths and distinct types of chemical bonds, film thickness, the difference between composites at the atomic scale, crystal stability, grain alignment, and size distribution. It is presently utilized to determine the structure of a wide range of biological compounds, including vitamins, pharmaceuticals, thin-film, and multi-layered materials. The most extensive application of it is to investigate precise ways in which the structure of a materials, medication, or chemical will interact in different surroundings [23].

## **RATIONALE**

This study aims to understand, simulate, and define different parameters of  $\text{Ga}_2\text{O}_3$  polymorphs by 3-D visualization. The main goal is to achieve better understanding of the crystal structures, XRD Patterns, fractional coordinates, and miller indices inserted lattice planes for  $\text{Ga}_2\text{O}_3$  polymorphs using VESTA Software. The results obtained from this study can be useful in the development of novel electronic and optical units, such as optoelectronics, sensors, and photovoltaic devices.

## OBJECTIVES

Following are the objectives of this study:

- To form the 3-D structures of  $\alpha$ - and  $\beta$ -Ga<sub>2</sub>O<sub>3</sub>
- To understand strategies used for visualization of atoms, ions and molecules.
- To visualize various aspects of Ga<sub>2</sub>O<sub>3</sub> polymorphs.
- To generate X-ray diffraction pattern from visualization of crystal structure.

## CHAPTER 2

### LITERATURE REVIEW

Jewel, M. U., et al (2023) presented point defects with functional exchange correlation in the corundum ( $\alpha$ ), monoclinic ( $\beta$ ), and orthorhombic ( $\gamma$ ) phases of  $\text{Ga}_2\text{O}_3$ . The Point defects inside several phases of  $\text{Ga}_2\text{O}_3$  comprised vacancies, antistites, and the extrinsic impurities. The energies of defect formation, transition energy levels, and the defect concentration fluctuations by temperature are reported and shown under the both Ga-rich as well as oxygen-rich development conditions. He formation energy diagrams show phases and the development of Ga/O vacancies with impurities. Charge transition levels are found deep within the bandgap, regardless of the  $\text{Ga}_2\text{O}_3$  phase or growth conditions. Vibrational modes of  $\beta\text{-Ga}_2\text{O}_3$  thin films are studied to examine the effects of temperature on intrinsic point defects.

Tang, X., et al (2023) stressed that gallium oxide gadgets are becoming progressively imperative in the world of electrical devices because of their unique characteristics. Gallium oxide as a semiconductor has a larger bandgap, dielectric constant and breakdown electric field than silicon. Furthermore, gallium oxide is a strong material that can withstand a wide range of temperatures and pressures, making it suited for hostile environments such as space or high temperatures. As a result, fabricating flexible  $\text{Ga}_2\text{O}_3$  devices directly on ordinary polymer substrates is problematic. In recent years, several manufacturing procedures, including as the transfer route, in situ room-temperature amorphous route, and in situ high-temperature epitaxy route, have been established in this field. They investigated the benefits and drawbacks of each strategy, as well as the prospects and challenges of adopting flexible  $\text{Ga}_2\text{O}_3$  device applications.

Zhu, Jun, et al. (2022) provided a complete evaluation of achievements in the field of  $\text{Ga}_2\text{O}_3$ -based gas sensors during the last thirty years. After discussing the various strategies, the authors highlighted the importance of understanding the sensing mechanism of  $\text{Ga}_2\text{O}_3$ -based gas sensors to further enhance their performance. They also suggested future directions for research in the field, particularly in developing novel v-based architectures and exploring new sensing applications.

Mondal, A. K., et al (2021) investigated the optical properties of pure  $\alpha$ -Ga<sub>2</sub>O<sub>3</sub> and Ca-doped  $\alpha$ -Ga<sub>2</sub>O<sub>3</sub>. By providing deep acceptor energy levels as an intermediate band above the valence band maximum, calcium (Ca) doping was identified to minimize the bandgap. Ca doping also enhances absorption while decreasing reflectance in the visible zone. Aside from that, when compared to pure material, transparency is reduced. Electron-photon inter-band transitions and the magnify function of the complex dielectric function were used to examine and explain optical properties.

Frodason, Y. K. (2021) investigated defects in the metal oxide semiconductors ZnO and Ga<sub>2</sub>O<sub>3</sub> by DFT. Hybrid functionals were employed for overcoming major limitations of the conventional XC functionals for describing defects in this materials system, namely the general underestimation of band gaps and delocalization error. The focus was on properties related to charge-state transitions involving defects, including defect luminescence, optical absorption and nonradiative capture and emission of charge carriers. Thermodynamic quantities such as defect formation energies and bonding emerge were also calculated in order to assess the likelihood of defect incorporation and the relative stability of defects and complexes. The results presented here show that hybrid functionals can provide a significantly improved description of defect properties such as the degree of charge localization and thermodynamic or optical charge-state transition energies, relative to conventional DFT. The comparison between first-principles calculations and experimental data has proven to be a fruitful approach in the study of defects in oxide semiconductors.

Swallow et al (2020) explored the electronic, structural and optical properties of  $\beta$ -Ga<sub>2</sub>O<sub>3</sub>, an extensive band-gap alternative to SiC and GaN. The study highlights the increasing importance of finding new materials to meet the advancing needs of energy efficient power electronics and the potential for  $\beta$ -Ga<sub>2</sub>O<sub>3</sub> to be a viable option. Through XRD and ab initio theoretical approaches, the researchers were able to investigate three polymorphs of Ga<sub>2</sub>O<sub>3</sub>. Their findings shed light on the relationship between the electronic structure and structure of the compounds.

Poncé, S., et al (2020) studied  $\beta$ -Ga<sub>2</sub>O<sub>3</sub>'s structural, and electrical properties. They discovered phonon frequencies as well as elastic constants that repeat the correct band ordering as observed in the experiment. They revealed that Ga<sub>2</sub>O<sub>3</sub> electron mobility of this

phase was caused by longitudinal-optical modes of Bu symmetry through a spectrum study of the scattering contribution to the inverse mobility. The breakdown field at room temperature was calculated to be 5.8 MV/cm, providing a Baliga figure of merit of 1250. This study laid the groundwork for future research into innovative high-power electronic materials.

L, K. H., (2020) stressed that current advancements in heterostructures based on gallium oxide have let optoelectronic devices to be utilize widely. The energy-bands are calculated using X-ray photoelectron spectroscopy at  $\beta$ -Ga<sub>2</sub>O<sub>3</sub>/ $\gamma$ -In<sub>2</sub>O<sub>3</sub> interface, explicating a type-heterojunction with conduction- and valence band offsets of 0.16 and 1.38 eV. It lays a strong basis for and paves the way to future all-oxide-based transparent photon platforms.

Roberts, J. W., et al. (2019) used triethyl gallium and the O<sub>2</sub> plasma to produce thin films of Ga<sub>2</sub>O<sub>3</sub> on sapphire substrates in the c-plane using plasma accelerated atom layer deposition. They looked at how substrate temperature and plasma dispensing parameters affected crystallinity and optical properties of Ga<sub>2</sub>O<sub>3</sub> films. The deposition temperature has a substantial impact on the crystallinity of the film. Temperatures less than 200°C were used to deposit amorphous Ga<sub>2</sub>O<sub>3</sub> films. Temperatures of 250°C to 350°C produced mostly  $\alpha$ -Ga<sub>2</sub>O<sub>3</sub> films. At temperatures above 350°C, the deposited films displayed a mixture of  $\alpha$ -Ga<sub>2</sub>O<sub>3</sub> and  $\epsilon$ -Ga<sub>2</sub>O<sub>3</sub> phases. UV transmittance measurements on Ga<sub>2</sub>O<sub>3</sub> films indicated bandgaps ranging from 5.0 eV to 5.2 eV, with the  $\alpha$ -Ga<sub>2</sub>O<sub>3</sub> phase having the largest bandgap at 250°C.

Sukapat, S. B. (2018) made-up by magnetron sputtering the high quality Ga<sub>2</sub>O<sub>3</sub> thin films to be used for fabricating the optoelectronic devices. The thin films were put on dual polished c-plane sapphire substrates. He did four investigations to enhance the superiority of thin films. Foremost, the result by using AR/O<sub>2</sub> mixture for the deposition was inspected. Secondly, the deposition annealing was explored where thin films were annealed in void and in changed gas environments. Thirdly, the outcome of changed substrate temperature from 20 C to 800 C was studied. The fourth examination was where Tn was presented in different amount to perform n-type doping of the films. Thin films of (2 0 1) oriented  $\beta$ -phase Ga<sub>2</sub>O<sub>3</sub> single crystal was obtained after deposition by using 100 % AR.

Yao, Y. et al (2019) analyzed the crystallinity in addition wafer uniformity of  $\beta$ -Ga<sub>2</sub>O<sub>3</sub> substrates oriented as (201) and (010) and inspected by the laboratory XRD, Raman spectroscopy, and mapping. The EFG substrates had the best crystallinity and uniformity, according to the data. The strand distribution predicted by Raman mapping called into doubt the homogeneity of both the (201) and (010) substrates. According to the findings, EFG-formed -Ga<sub>2</sub>O<sub>3</sub> ingots show high crystallinity and can be considered three-dimensionally uniform bulk crystals for both undoped and Sn-doped growth.

Ratter, J. R. (2019) presented magnesium doped Ga<sub>2</sub>O<sub>3</sub> for creating a semiconducting material, to be utilized in very high-powered devices.  $\beta$ -Ga<sub>2</sub>O<sub>3</sub> *which is not* doped and Ca-doped  $\beta$ -Ga<sub>2</sub>O<sub>3</sub>, IR peaks are allotted to O–H bond that stretch IrH modes complexes. For Ga<sub>2</sub>O<sub>3</sub> which is hydrogen-annealed: He used polarization experiments for placing the O-H bond of the MH complex in the *a-c* plane. When the intensity of this feature vs photoexcitation was examined, the donor level was 2.2-2.3 eV under conduction band minimum. Ga<sub>2</sub>O<sub>3</sub>: Mg has sidebands ranging from 5100 to 5200 cm<sup>-1</sup>.

Michl, G. et al (2017) offered a 3D game which is developed with Unity3D. The player thus has control of an electron hovering within the crystal. Though, this flight over the crystal is not unrestricted from hindrances. In the central of the structure there are steadily existing oxide layers which, if the electrons speed is too low, avoid the passage and resist the electron. Just at high-speed it can tunnel through them. Though, the attention was on the datum that the user can fine-tune the scene and can generate all probable semiconductor structures which is not only fine for observing and acknowledging diverse structural shapes and their symmetries, but also for playing experience. The applications based on cellVIEW, a stratagem for the imagining of widespread molecular structures, which allows us to execute high-performance execution of semiconductor structures of atoms often far more than fifteen million.

Stepanov, S., et al (2016) concluded the work directed in the area of TCO gallium oxide. To attain the exacting standards of purity and defect density required for semiconductor applications, maximum of research and development struggle has been taken on. Polymorphism, band-structure, and opto-electrical properties of Gallium Oxide was investigated by him while emphasizing on the different methods for making the thin films

of  $\text{Ga}_2\text{O}_3$  and bulk crystals. Gallium oxide has gained significant concentration as a handy substance for many appliances.

Masataka Hgashwak et al (2014) were able to successfully produce high-quality epitaxial thin films of gallium oxide that were n-type using ozone molecular beam epitaxy, resulting in thin films with manageable carrier densities. The devices exhibited promising properties using ozone molecular beam epitaxy, resulting in manageable carrier densities. From these films, they made-up  $\text{Ga}_2\text{O}_3$  transistors and Schottky diodes, using both single-crystal substrates and epitaxial wafers grown via MBE. These devices exhibited desirable traits, including high reverse voltage breakdown, suggesting that gallium oxide could outperform wide band gap semiconductors like Si or GaN in certain applications.

L, Land et al (2012) demonstrated that the method used to synthesize  $\alpha$ ,  $\beta$ , and  $\gamma$ - $\text{Ga}_2\text{O}_3$  is a scalable one, which involves using an aqueous solution of gallium nitrate and sodium carbonate without the need for surfactants or additives. Two calcination processes were used to obtain  $\alpha$ -Ga OH, which was prepared by a controlled precipitation at a constant pH uses an aqueous solution of gallium nitrate and sodium carbonate without the need for surfactants or additives. The  $\alpha$  and  $\beta$ - $\text{Ga}_2\text{O}_3$  variants were obtained through the calcination of  $\alpha$ -Ga OH, which was prepared by precisely controlling the pH at 6 and a constant temperature of  $55^\circ\text{C}$  for 24 hours during the precipitation process. On the other hand,  $\gamma$ - $\text{Ga}_2\text{O}_3$  was obtained by calcining the Gallia gel, which was synthesized at a constant pH of 4 and temperature of  $25^\circ\text{C}$  without the need for any further processing. Overall, this synthesis approach provides a promising avenue for cost-effective and scalable production of  $\alpha$ ,  $\beta$ , and  $\gamma$ - $\text{Ga}_2\text{O}_3$ , which can offer numerous application opportunities for  $\text{Ga}_2\text{O}_3$ -based materials and devices. The use of a simple and efficient process without the need for additional reagents or surfactants makes this method a viable option for commercial production in the future.

# CHAPTER 3

## METHODOLOGY

### 3.1 Visualization for Electronic and Structural Analysis (VESTA)

#### 3.1.1 Introduction

VESTA is a powerful software tool that enables researchers to visualize and analyze a wide range of structural information in a highly flexible and customizable manner. With its user-friendly interface and intuitive tools, VESTA allows researchers to explore structural information with a high degree of detail and precision. The software provides a range of visualization options, including ball-and-stick, space-filling, and polyhedral representations, as well as customizable color coding and labeling. Additionally, VESTA offers a variety of calculation and plotting capabilities, allowing scientists to analyze and visualize structural properties such as bond distances, angles, and torsion angles, as well as interatomic distances and angles between planes [25].

Overall, VESTA is an essential tool for any scientist studying crystal structures, materials properties, chemical bonding, and related fields. Its ability to handle large volumes of complex data and provide a range of visualization and analytical options makes it an indispensable resource for researchers in both academia and industry [25].

#### 3.1.2 Features of VESTA

- VESTA is a versatile software that can operate on multiple operating systems including Windows, Mac OS X, and Linux.
- It offers a range of useful features such as crystal morphology visualization, powder X-ray diffraction simulations, and isosurfaces visualization with multiple levels.
- Additionally, VESTA has a Powder X-Ray diffraction simulator which allows users to investigate the diffraction patterns of materials.
- Furthermore, VESTA includes the feature of electron and nuclear densities integration via Voronoi tessellation which assists in advanced analyses.

- Finally, VESTA has significantly improved its performance in isosurfaces rendering and slice calculations, providing users with faster and more accurate results [26].

### **3.1.3 Visualization of Structural Models**

VESTA represents crystal structures as:

- Ball & stick
- Space filling
- Polyhedral
- Stick
- Wireframe [27].

### **3.2 Display Crystallographic Information**

Provision of variety of crystallographic information such as:

- Fractional coordinates,
- Symmetry operations and translation vectors,
- Site multiplicities, Wyckoff letters, and site symmetry,
- Interatomic distances, bond angles, and torsion angles [27].

### **3.3 Lattice Transformation**

VESTA possesses the ability to convert general equivalent positions in a consistent configuration into those in an unconventional one, using a transformation matrix. This same matrix can also be utilized for converting primitive lattice structures into complex lattice structures, as well as generating superstructures. This feature greatly enhances VESTA's versatility in handling various types of crystal structures and supports the study of materials science through efficient and accurate conversions [27].

### **3.4 Dealing with Volumetric Data**

#### **3.4.1 Visualization of Volumetric Data**

Rendered as a color gradient, or with different colors assigned to positive and negative values. Isosurfaces are commonly used in scientific visualization and provide an effective and intuitive way to represent the shape and distribution of 3D data sets, such as molecular structures and geological formations. By utilizing various visualization techniques, such as

smooth-shaded polygons, wireframes, and dot surfaces, isosurfaces powerful way to represent three-dimensional data in a manner that is easily interpretable by researchers and scientists. By representing physical quantities using isosurfaces with different colors or shading, it is possible to visualize the distribution and magnitude of the physical quantity in question. This allows for a deeper understanding of the underlying physics of a system and can facilitate the development of new theories and models to explain the observed behavior [27].

### **3.4.2 Pixel operation of multiple 3D Data**

In addition to the ability to perform pixel operations between multiple 3D data sets, VESTA also supports the multiplication of an arbitrary factor to each data set. One potential application of this feature is the detection of light atoms that are missing in a structural model. This feature enables various scientific applications, such as the subtraction of calculated electron densities from observed ones obtained by MEM analysis to identify light atoms that are missing in a structural model. By multiplying a scaling factor to each 3D data set, VESTA allows researchers to fine-tune the visualization of data and gain insights into the relationships and interactions between different physical phenomena. Furthermore, the ability to perform pixel operations between more than two 3D data sets provides greater flexibility and versatility in analyzing complex data sets from different sources and experimental techniques. Overall, VESTA's advanced capabilities and user-friendly interface make it a valuable tool for researchers in materials science, chemistry, geology, and other fields requiring 3D visualization and analysis of structural and compositional data [27].

### **3.4.3 Surface Coloring**

This feature can also be used to colorize isosurfaces of other physical quantities, such as temperature, magnetization, or any other parameter of interest. The peak values and any other scalar field associated with the crystal structure. Additionally, VESTA provides the ability to list peak values and positions in the Text Area, which can be used for more detailed analysis and interpretation of the data. By enabling users to colorize isosurfaces, VESTA facilitates the visualization and analysis of complex 3D data sets in various scientific disciplines, including materials science, chemistry, and physics. To summarize, VESTA's isosurfaces colorization feature is a powerful tool that enables users to visualize

and analyze complex 3D data sets in a more meaningful way, helping to advance scientific research in a variety of fields [27].

### 3.4.4 Display Lattice Planes and Crystal Morphologies

This is valuable for analyzing crystal symmetry and identifying defects or irregularities in the lattice. By allowing users to insert lattice planes with variable opacities, VESTA provides greater flexibility in visualizing and manipulating crystal structures. This within the crystal structure, which are useful for determining crystal symmetry, identifying defects and impurities, and characterizing the properties of crystalline materials. By incorporating variable opacities into lattice planes, VESTA enables researchers to highlight specific features within the crystal structure and gain a deeper understanding of their role in material properties and behavior. Overall, VESTA's ability to colorize and manipulate 3D pixel data, draw crystal morphologies, and measure distances and angles within the crystal structure, enables researchers to more effectively analyze and interpret complex materials data, and ultimately advance our understanding of the underlying physics and chemistry that govern their behavior [27].

## 3.5 Construction of Structure of $\alpha\text{-Ga}_2\text{O}_3$

### 3.5.1 Main Window

By opening the VESTA software, the Main Window appears as shown in figure 3.1.



Figure 3. 1 Main Window

### 3.5.2 Unit Cell

To make the crystal structure, click on 'File' on the Menu Bar then on 'New Structure' add the title in the phase and then click 'Unit Cell'.

### 3.5.3 Selecting Parameters

After clicking the unit cell, select the 'symmetry' and 'lattice parameters' as shown in figure for construction of monoclinic  $\alpha$ -Ga<sub>2</sub>O<sub>3</sub> crystal structure in 3-dimensions.

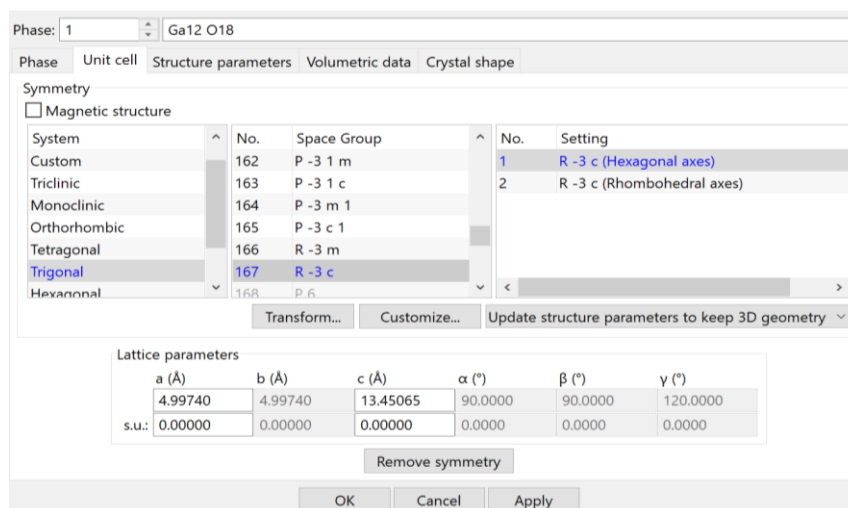


Figure 3. 2 Selecting Structural Parameters for  $\alpha$ -Ga<sub>2</sub>O<sub>3</sub>

To execute click on 'apply' and then 'Ok'.

## 3.6 Construction of Structure of $\beta$ -Ga<sub>2</sub>O<sub>3</sub>

### 3.6.1 Main Window

The first step is to open the VESTA Software then the 'Main Window' appears as shown in figure 3.1.

### 3.6.2 Unit Cell

With the purpose of constructing the crystal structure of  $\beta$ -Ga<sub>2</sub>O<sub>3</sub>, click 'File' on the Main Window top bar then on 'New Structure' add the title in the phase and then click 'Unit Cell'.

### 3.6.3 Selecting Parameters

After clicking the unit cell, select the 'symmetry' and 'lattice parameters' as shown in figure for construction of monoclinic  $\beta$ -Ga<sub>2</sub>O<sub>3</sub> crystal structure in 3-dimensions.

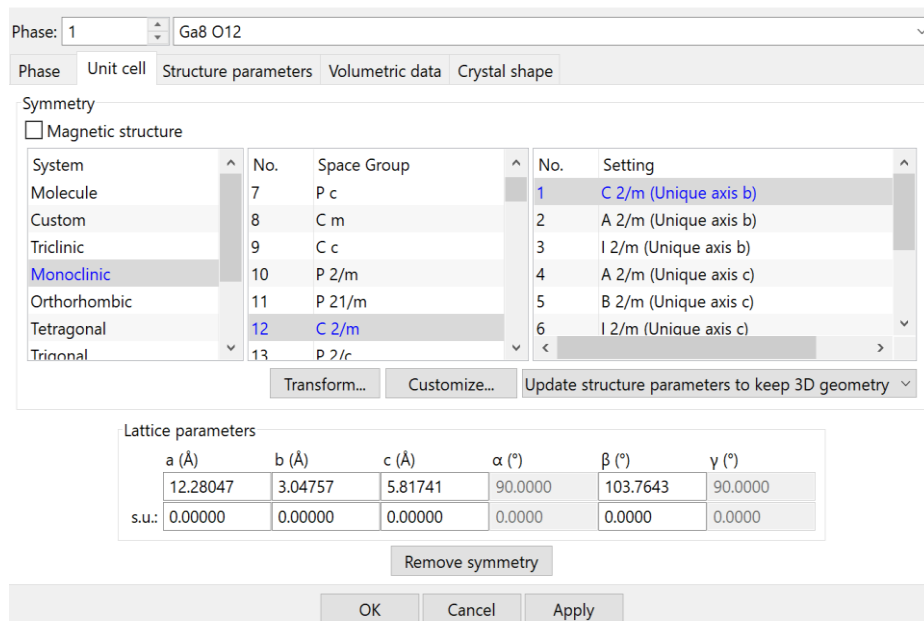


Figure 3.3 Structural parameters for  $\beta$ - $Ga_2O_3$

### 3.7 Crystal Structure Models

Following five different models are displayed for both phases of  $Ga_2O_3$  to make their crystal structures using VESTA Software as shown in Figure 3.5.

- Ball and Stick
- Stick Models
- Polyhedral
- Wireframe
- Space filling

#### 3.7.1 Ball-and-stick

In the “Ball-and-stick” model, all the atoms are articulated as solid spheres. Bonds are articulated as either cylinders or the lines [27].

#### 3.7.2 Space-filling

In the “Space-filling” model, atoms are drawn as interpenetrating solid spheres, with radii stated at the Atoms tab option in the Properties dialog box [27].

#### 3.7.3 Polyhedral

The polyhedral model is a useful tool for visualizing complex crystal structures and identifying key features such as bond angles and coordination numbers. By including central atoms, bonds, and apex atoms, the model provides a comprehensive view of the crystal structure and allows for detailed analysis of the chemical bonding and geometry within the lattice. The Bonds dialog box allows users to selectively display specific bonds, highlighting critical interactions between atoms and providing valuable insights into the structure-property relationships of the material. The polyhedral model is a versatile and powerful tool for analyzing crystal structures, and when combined with other visualization and analysis techniques, can greatly enhance our understanding of the underlying physics and chemistry of materials [27].

### 3.7.4 Wireframe

In the “Wireframe” model, atoms having no bonds are drawn as wire-frame spheres whereas those bonded to other atoms are never drawn. All the bonds are presented as lines with gradient colors [27].

### 3.7.5 Stick

Atoms with no bonds are drawn in the “Stick” model as solid spheres while the atoms bonded to other atoms are not drawn. The bonds are shown as cylinders, whose properties can be changed at the Bonds tab in the Properties dialog box [27].

## 3.8 Lattice Planes

### 3.8.1 Interplanar Distances

For insertion of the lattice planes, first step is to calculate the interplanar distance between Miller Indices’ three adjacent values for both phases of gallium oxide. The spacing  $d$  between these planes in trigonal crystals of  $\alpha$ -Ga<sub>2</sub>O<sub>3</sub> with lattice constant  $a$  is calculated by formula:

$$\frac{1}{d^2} = \frac{(h^2 + k^2 + l^2) \sin^2 \alpha + 2(hk + kl + hl)(\cos^2 \alpha - \cos \alpha)}{a^2(1 - 3 \cos^2 \alpha + 2 \cos^3 \alpha)}$$

While on the other hand spacing  $d$  between lattice planes in monoclinic  $\beta$ -Ga<sub>2</sub>O<sub>3</sub> is calculated by formula:

$$\frac{1}{d^2} = \frac{1}{\sin^2 \beta} \left( \frac{h^2}{a^2} + \frac{k^2 \sin^2 \beta}{b^2} + \frac{l^2}{c^2} - \frac{2hl \cos \beta}{ac} \right)$$

### 3.8.2 Lattice Planes Insertion in $\alpha$ -Ga<sub>2</sub>O<sub>3</sub> Unit Cell

Click on the 'Edit' on the top menu bar to insert lattice planes in unit cell of  $\alpha$ -Ga<sub>2</sub>O<sub>3</sub> and then select 'Lattice Planes' as shown in the figure below.

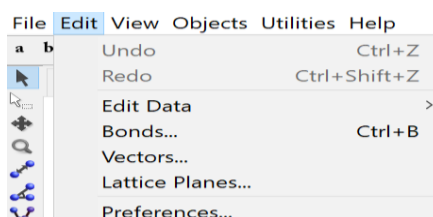


Figure 3.4 Inserting Lattice Planes

A small box will appear after clicking 'Lattice Planes' where the values will be inserted accordingly for each lattice planes with inter planar distance  $d$  as shown in the figure.

### 3.8.3 Lattice Planes for $\beta$ -Ga<sub>2</sub>O<sub>3</sub>

Click on the 'Edit' on the top menu bar to insert lattice planes in unit cell of  $\beta$ -Ga<sub>2</sub>O<sub>3</sub> and then select 'Lattice Planes'. A small box will appear after clicking 'Lattice Planes' where the values will be inserted accordingly for each lattice planes with inter planar distance  $d$ .

## 3.9 Range of Fractional Coordinates

### 3.9.1 In case of $\alpha$ -Ga<sub>2</sub>O<sub>3</sub>

Ranges of fractional coordinate can be determined by clicking on the icon 'Boundary' at the left most corner of Main Window. Then we can edit the ranges of fractional coordinate and put the values accordingly.

### 3.9.2 In case of $\beta$ -Ga<sub>2</sub>O<sub>3</sub>

Ranges of fractional coordinate can be determined by clicking on the icon 'Boundary' at the left most corner of Main Window. Then we can edit the ranges of fractional coordinate and put the values accordingly.

## 3.10 Powder Diffraction Patterns

Click on the 'Utilities' from top bar in the Main Window to find the powder diffraction pattern for both phases of gallium oxide. A list of options will appear from which selecting

the 'Powder Diffraction Patterns' will give the graphical representation of required crystal structure. Then click 'Calculate'.

## CHAPTER 4

### RESULTS AND DISCUSSION

#### 4.1 Crystallographic Models for $\alpha\text{-Ga}_2\text{O}_3$

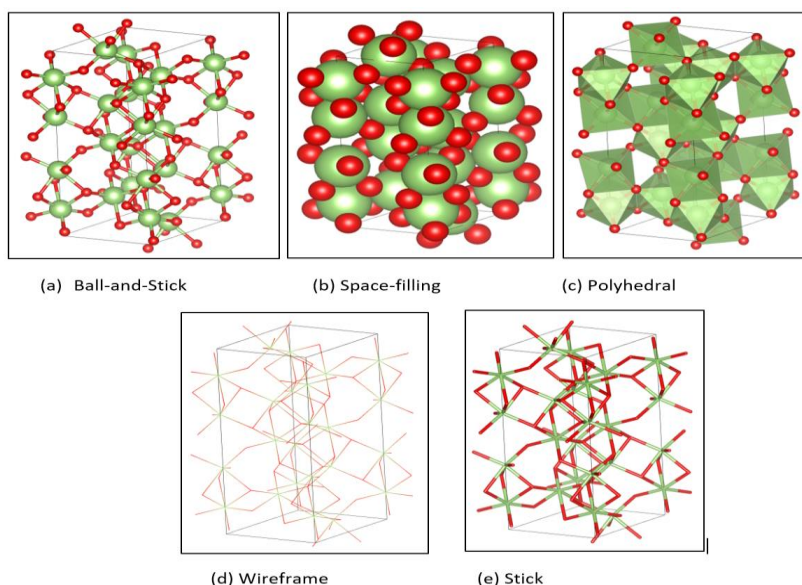


Figure 4.1  $\alpha\text{-Ga}_2\text{O}_3$  Crystallographic Models

Models in terms of crystallographic representation of trigonal  $\alpha\text{-Ga}_2\text{O}_3$  polymorph are shown in Figure 4.1. Color Code is Red and Green. Green sticks and spheres represent Gallium (Ga) atoms while red sticks and spheres represents Oxygen (O) atoms.

Figure 4.1 (a) shows a Ball-and-Stick structure that represents the atoms as solid spheres where bonds are represented as lines. Figure 4.1 (b) shows space-filling structure that represents atomic size of Gallium is larger than Oxygen. Figure 4.1 (c) shows Polyhedral structure that shows the atoms as solid spheres and the bonds as either cylinders or lines. Figure 4.1 (d) shows wireframe structure that represents the structure in wire form with no balls and sticks. Figure 4.1 (e) shows Stick model that represents only stick as bond between Ga and O. Atoms are represented in different colors in order to differentiate from each other to make visualization of atoms and molecules easy to comprehend and estimate various aspects of crystal structure. Calculated values are in good agreement with previously reported values.

## 4.2 Crystallographic Models for $\beta\text{-Ga}_2\text{O}_3$

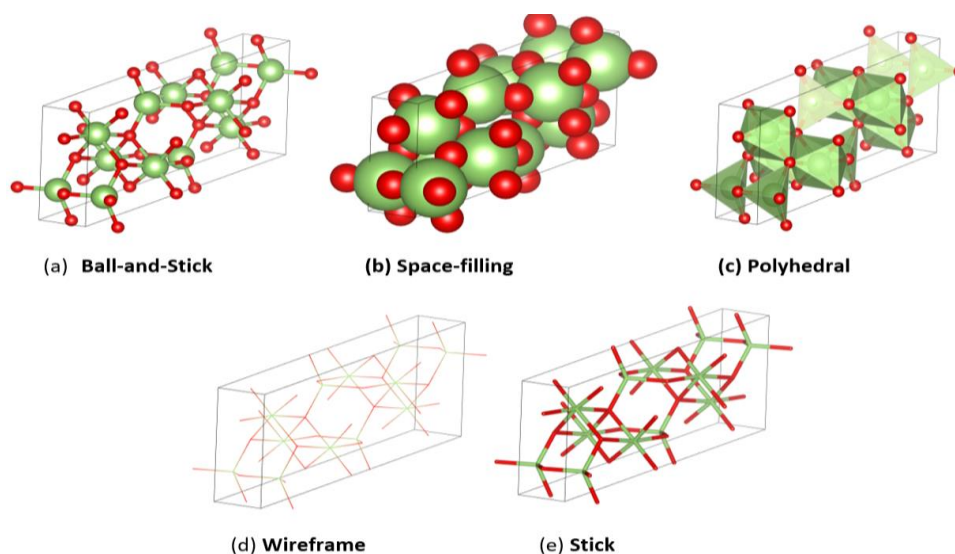


Figure 4.2  $\beta\text{-Ga}_2\text{O}_3$  Crystallographic Models

Models in terms of crystallographic representation of monoclinic  $\beta\text{-Ga}_2\text{O}_3$  polymorph are shown in Figure 4.2. Color Code is Red and Green. Green sticks and spheres represent Gallium (Ga) atoms while red sticks and spheres represents Oxygen (O) atoms.

Figure 4.2 (a) shows a Ball-and-Stick structure that represents the atoms as solid spheres or ellipsoids where bonds are represented as or lines. Figure 4.2 (b) shows space-filling structure that represents atomic size of Gallium is larger than Oxygen. Figure 4.2 (c) shows Polyhedral structure that shows the atoms as solid spheres and the bonds as either cylinders or lines. Figure 4.2 (d) shows wireframe structure that represents the structure in wire form with no balls and sticks. Figure 4.2 (e) shows Stick model that represents only stick as bond between Ga and O. Atoms are represented in different colors in order to distinguish from each other to make visualization of atoms and molecules easy to understand and estimate various aspects of crystal structure. Calculated values are in good agreement with previously reported values.

### 4.3 Ranges of Fractional Coordinates for $\alpha$ -Ga<sub>2</sub>O<sub>3</sub>

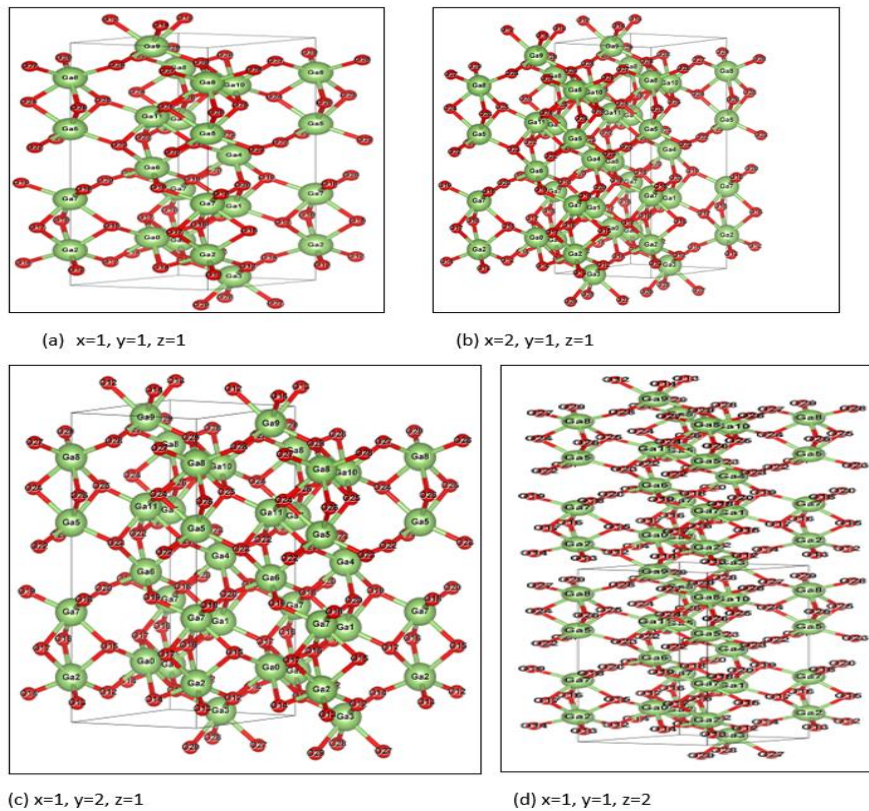


Figure 4. 3 Ranges of Fractional Coordinates in  $\alpha$ -Ga<sub>2</sub>O<sub>3</sub>

In Figure 4.3 crystallographic representation in terms of fractional coordinates are shown for trigonal  $\alpha$ -Ga<sub>2</sub>O<sub>3</sub> polymorphs. Color Code is Red and Green. Green sticks and spheres represent Gallium (Ga) atoms while red sticks and spheres represents Oxygen (O) atoms.

Figure 4.3 (a) illustrates ball and stick model for trigonal  $\alpha$ -Ga<sub>2</sub>O<sub>3</sub> that have  $x=1, y=1, z=1$  representing that there is only one unit cell and no transition along any axes. Figure 4.3 (b) represents range of fractional coordinates  $x=2, y=1, z=1$  representing an additional unit cell along x axes and transition of atoms along this axe. Figure 4.3 (c) represents range of fractional coordinates  $x=1, y=2, z=1$  representing an additional unit cell along any axes and transition of atoms along this axe. Figure 4.3 (d) represents range of fractional coordinates  $x=1, y=1, z=2$  representing an additional unit cell along z axes and transition of atoms along this axe.

#### 4.4 Ranges of Fractional Coordinates for $\beta - \text{Ga}_2\text{O}_3$

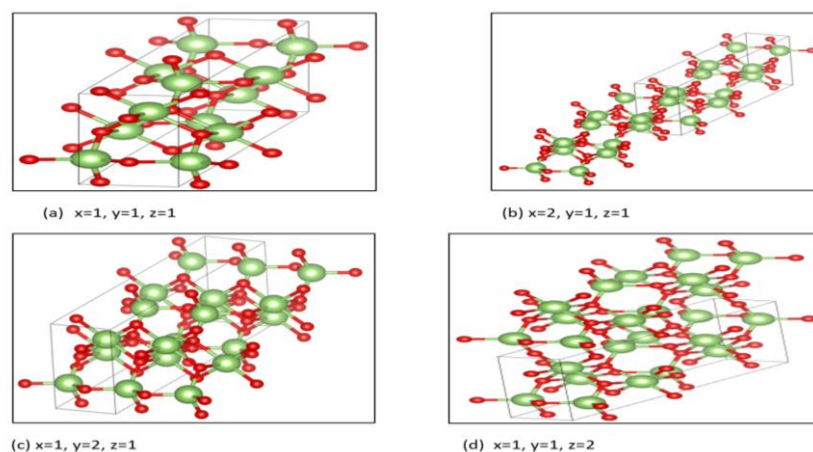


Figure 4.4 Ranges of Fractional Coordinates in  $\beta\text{-Ga}_2\text{O}_3$

In Figure 4.4 crystallographic representation in terms of fractional coordinates are shown for monoclinic  $\beta\text{-Ga}_2\text{O}_3$  polymorphs. Color Code is Red and Green. Green sticks and spheres represent Gallium (Ga) atoms while red sticks and spheres represents Oxygen (O) atoms.

Figure 4.4 (a) illustrates ball and stick model for monoclinic  $\beta\text{-Ga}_2\text{O}_3$  that have  $x=1, y=1, z=1$  representing that there is only one unit cell and no transition along any axes. Figure 4.4 (b) represents range of fractional coordinates  $x=2, y=1, z=1$  representing an additional unit cell along x axes and transition of atoms along this axis. Figure 4.4 (c) represents range of fractional coordinates  $x=1, y=2, z=1$  representing an additional unit cell along any axes and transition of atoms along this axis. Figure 4.4 (d) represents range of fractional coordinates  $x=1, y=1, z=2$  representing an additional unit cell along z axes and transition of atoms along this axis.

Changing the ranges of fractional coordinates causes the number of atoms in a crystal compound to differ because fractional coordinate represents the relative position of atom in the crystal lattice. When the range is changed the relative position of atom is also changed. This results in addition or removal of atom, the number of atoms from the crystal structure as well arrangement of atoms within the lattice. Thus, it has a significant impact on the composition and properties of crystal structure.

#### 4.5 Lattice Planes for $\alpha\text{-Ga}_2\text{O}_3$

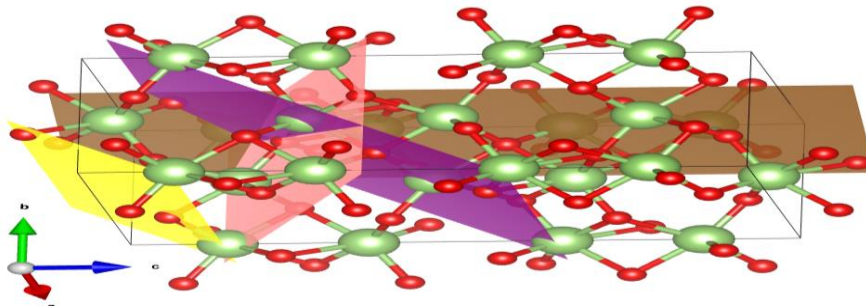


Figure 4. 5 Lattice planes with different Miller Indices

Figure 4.5 shows crystallographic representation in terms of lattice planes. Purple color represents (024) plane. Yellow color represents (012) planes. Peach color shows (104) plane and brown shows (110) plane. Figures show different miller indices (hkl) vales with different lattice planes and distance from origin for trigonal  $\text{Ga}_2\text{O}_3$ . The planes are represented in different colors to distinguish from each other. These lattice planes are inserted in trigonal alpha gallium oxide crystal structure. Each lattice plane contains set of three miller index notation. By changing the miller indices, the dimensions of lattice planes in crystal structure also changed.

#### 4.6 Lattice planes for $\beta\text{-Ga}_2\text{O}_3$

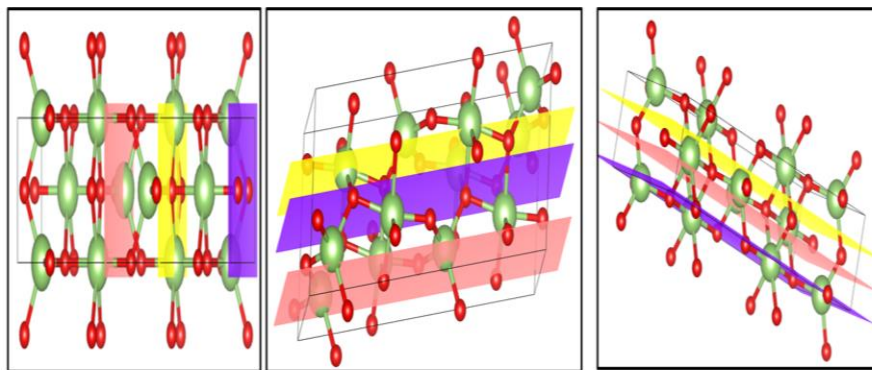


Figure 4.6 Planes with different indices

Figure 4.6 shows crystallographic representation in terms of lattice planes. Purple color represents (100) (001) and (010) planes. Yellow color represents (200) (002) and (020) planes. Peach color represents (300) (003) and (030) planes.

Figures show different miller indices (hkl) vales with different lattice planes and distance from origin for monoclinic  $\beta\text{-Ga}_2\text{O}_3$ . The planes are represented in different colors to

distinguish from each other. These lattice planes are inserted in trigonal alpha gallium oxide crystal structure. Each lattice plane contains set of three miller index notation. By changing the miller indices, the dimensions of lattice planes in crystal structure also changed.

#### 4.7 Powder Diffraction Pattern for $\alpha\text{-Ga}_2\text{O}_3$

Figure 4.7 shows the most intense lattice planes of  $\alpha\text{-Ga}_2\text{O}_3$  by using powder diffraction (XRD) pattern. This graph characterizes intensity on y-axis and the angle  $2\theta$  on the x-axis. The highest peak appears at most penetrating lattice planes with (h k l) values of (104) at an angle of  $100^\circ$ . (110) appears in powder diffraction pattern graph at an angle of  $78^\circ$ . (012) peak appears at  $32^\circ$  angle while (024) peak appear at an angle of  $29^\circ$ . It characterizes x-ray powder diffraction pattern (XRD) for trigonal  $\alpha\text{-Ga}_2\text{O}_3$  polymorph. The peaks occurring at  $2\theta$  exhibits most intense lattice planes with (h k l) values of (104), (110), (012) and (024) planes.

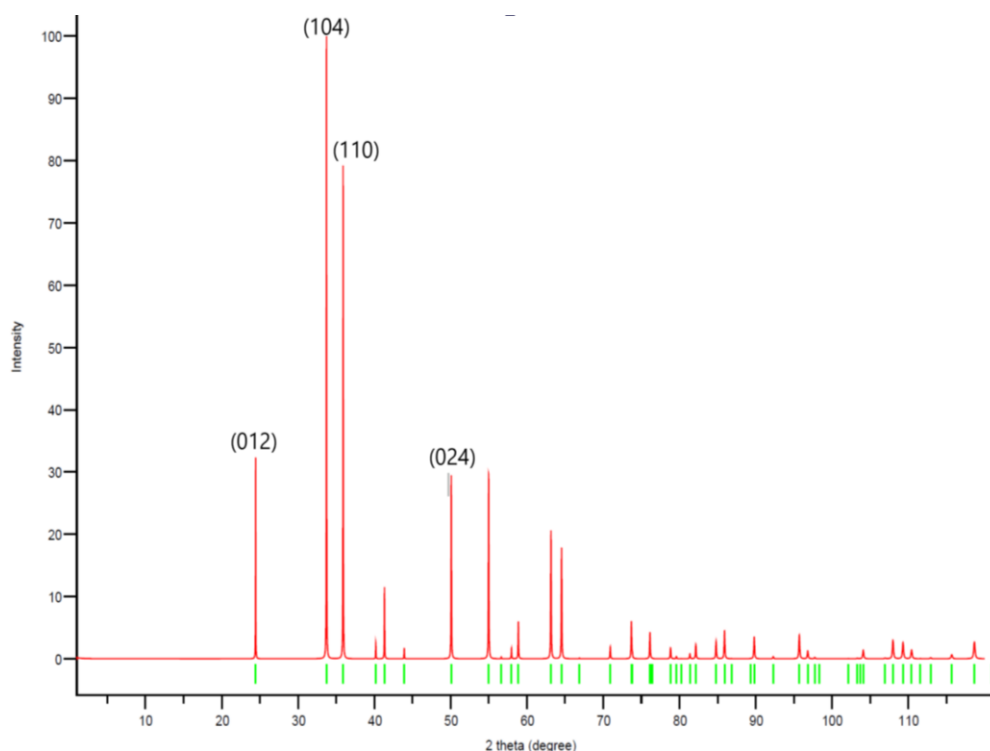


Figure 4.7 XRD Pattern for  $\alpha\text{-Ga}_2\text{O}_3$

The products are highly crystalline, as seen by the narrow sharp peaks. From the graph we observed the most dominant miller index (104). Because when x-rays fall on the crystal sample of  $\alpha\text{-Ga}_2\text{O}_3$  the most intense rays detected at  $2\theta$  angle is (104) miller index. These values are in good agreement with the previously specified figures.

#### 4.8 Powder Diffraction Pattern for $\beta\text{-Ga}_2\text{O}_3$

Figure 4.8 shows the most penetrating lattice planes of  $\beta\text{-Ga}_2\text{O}_3$  through the powder diffraction (XRD) pattern. This graph characterizes intensity on y-axis and the angle  $2\theta$  on the x-axis. The highest peak appears at most penetrating lattice planes with (h k l) values of (002) at an angle of  $100^\circ$ . (111) appears in powder diffraction pattern graph at an angle of  $88.6^\circ$ . (401) peak appears at  $59^\circ$ . It characterizes x-ray powder diffraction pattern (XRD) for  $\beta\text{-Ga}_2\text{O}_3$  polymorph. The peaks occurring at  $2\theta$  exhibits most intense lattice planes with (h k l) values of (002), (111) and (401) planes.

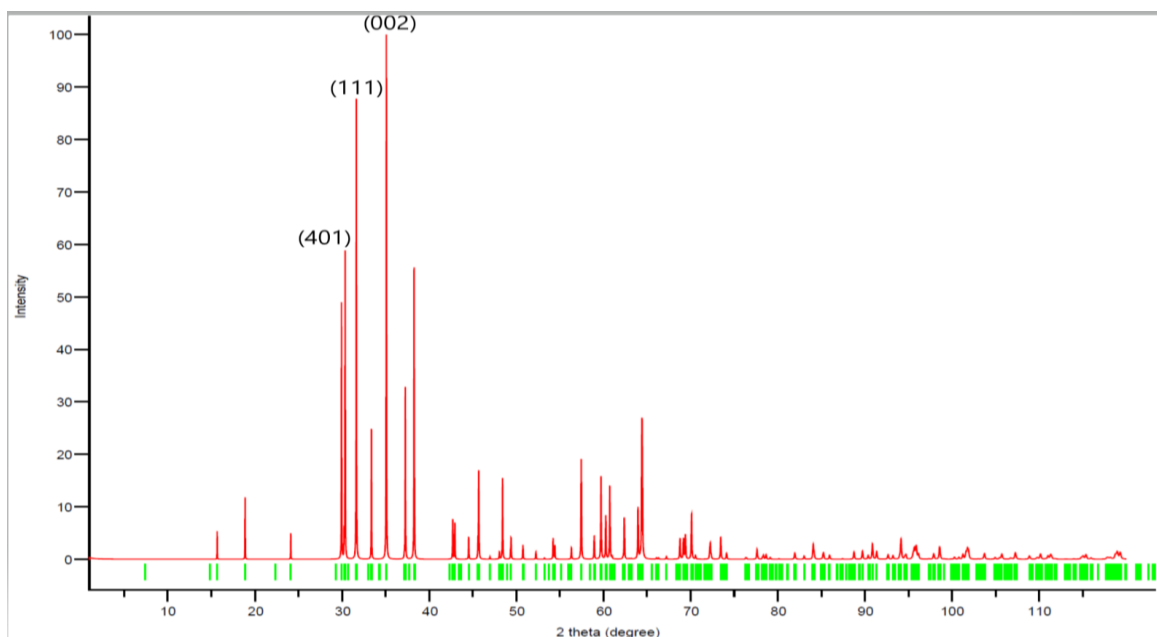


Figure 4.8 XRD Pattern for  $\beta\text{-Ga}_2\text{O}_3$

The products are highly crystalline, as seen by the narrow sharp peaks. From the graph we observed the most dominant miller index (002). Because when x-rays fall on the crystal sample of  $\beta\text{-Ga}_2\text{O}_3$  the most intense rays detected at  $2\theta$  angle is (002) miller index. These values are in good agreement with the previously specified figures.

Table 4.1 Lattice Parameters and Atomic Positions for  $\alpha\text{-Ga}_2\text{O}_3$

Crystallographic Parameters						Atomic Positions				Bond Length	
Axis Å			Angle			Atom	x	y	z	Calculated length Å	Referenced value [2] Å
a	b	c	A	$\beta$	$\gamma$						
4.98	4.98	13.5	90	90	120	Ga	0.00	0	0.1444		
						O	0.00	0.303167	0.250000		

Table 4.2 Unit Cell Parameters and Atomic Positions for  $\beta\text{-Ga}_2\text{O}_3$

Crystallographic Parameters						Atomic Positions				Bond Length	
Axis Å			Angle			Atom	X	y	z	Calculated length Å	Referenced value Å [20]
a	b	c	$\alpha$	$\beta$	$\gamma$						
12.28	3.05	5.82	90	103.8	90	Ga	0.090474	0	0.7948		
						Ga	0.158838	0.5	0.3147		
						O	0.003531	0.5	0.7433		
						O	0.16451	0.5	0.1091		
						O	0.17337	0	0.5632		

## CONCLUSION

Two polymorphs  $\alpha$ -Ga<sub>2</sub>O<sub>3</sub> and  $\beta$ -Ga<sub>2</sub>O<sub>3</sub> are investigated in terms of their crystallographic characteristics. Crystal structure models of  $\alpha$ - and  $\beta$ -Ga<sub>2</sub>O<sub>3</sub> visualized as polyhedral, wireframe, space filling and stick forms for better understanding of atomic models by using VESTA. Crystallographic representations in terms of fractional coordinates are also visualized by 3D structures and have studied their behavior in respective fractional coordinates. Lattice planes and Powder diffraction patterns (XRD) are also generated for both phases. For  $\alpha$  the highest peaks occur at plane of (104) while on the other hand  $\beta$  shows highest peak at (002) plane. The bond length of Ga with Oxygen atoms was estimated in Angstroms (Å). The bond length Between Ga and oxygen O was 2.186 Å while bond length between Ga and O in case of beta was 2.19 Å and all the values were in good agreement with previously investigated values. Monoclinic  $\beta$ -phase is the most stable polymorph, which associates amplified band gap with the enhanced conduction and breakdown field, along with better transparency in the UV spectral range. This VESTA tool may be used to analyze electron/nucleus density for a variety of the transition metal oxide-based polymorphs nanomaterials.

## LIMITATIONS

- VESTA has limited functionality when it comes to conducting complex calculations such as density functional theory (DFT) calculations or phonon calculations. As VESTA lacks some advanced features, it may not be suitable for certain types of research where high-level calculations or simulations are required. These advanced calculations are crucial for understanding the electronic and phonon properties of materials, which are important for predicting their behavior in various applications.
- Moreover, VASP and WIEN2K software offer more advanced features such as the ability to perform DFT calculations and calculate electronic band structures, which are essential for predicting the electronic, magnetic, and optical properties of materials.
- Furthermore, VASP and WIEN2K software have better accuracy and reliability when it comes to predicting the properties of materials. This is due to the more advanced algorithms and computational methods implemented in these software packages.
- Therefore, while VESTA is a powerful and useful tool for visualizing crystal structures and obtaining certain properties of materials, it cannot replace the more advanced paid software such as VASP and WIEN2K for conducting comprehensive studies on the electronic and phonon properties of materials.

## REFERENCES

[1] Crystalline Solids Available from:

<https://www.chem.fsu.edu/chemlab/chm1046course/solids.html> [cited September 15, 2022].

[2] Mondal, A. K., Mohamed, M. A., Ping, L. K., Mohamad Taib, M. F., Samat, M. H., Mohammad Haniff, M. A. S., & Bahru, R. (2021). First-Principles Studies for Electronic Structure and Optical Properties of p-Type Calcium Doped  $\alpha$ -Ga<sub>2</sub>O<sub>3</sub>. *Materials* 2021, 14, 604.

[3] Unit Cell Available from:

[https://www.doitpoms.ac.uk/tlplib/crystallography3/unit\\_cell.php](https://www.doitpoms.ac.uk/tlplib/crystallography3/unit_cell.php) [November 2, 2022].

[4] Crystal Structure. Available from:

[https://en.wikipedia.org/wiki/Crystal\\_structure](https://en.wikipedia.org/wiki/Crystal_structure) [November 29, 2022].

[5] Crystal Structure. Available from:

[https://chem.libretexts.org/Crystal\\_structure](https://chem.libretexts.org/Crystal_structure) [cited November 9, 2022].

[6] Da Silva, J. L., Walsh, A., & Wei, S. H. (2009). Theoretical investigation of atomic and electronic structures of Ga<sub>2</sub>O<sub>3</sub> (ZnO)<sub>6</sub>. *Physical Review B*, 80(21), 214118.

[7] Zhu, J., Xu, Z., Ha, S., Li, D., Zhang, K., Zhang, H., & Feng, J. (2022). Gallium Oxide for Gas Sensor Applications: A Comprehensive Review. *Materials*, 15(20), 7339.

[8] Periodic table. Available from:

[https://en.wikipedia.org/wiki/Periodic\\_table#:~:text=Today%20%2018%20elements%20are%20known,of%20which%20occur%20in%20nature](https://en.wikipedia.org/wiki/Periodic_table#:~:text=Today%20%2018%20elements%20are%20known,of%20which%20occur%20in%20nature) [cited December 26, 2022].

[9] Zhu, J., Xu, Z., Ha, S., Li, D., Zhang, K., Zhang, H., & Feng, J. (2022). Gallium Oxide for Gas Sensor Applications: A Comprehensive Review. *Materials*, 15(20), 7339.

[10] Oxides Available from:

<https://en.wikipedia.org/wiki/Oxide> [cited January 9, 2023].

[11] Tang, X., Lu, Y., & Li, X. (2023). Flexible gallium oxide electronics. *Semiconductor Science and Technology*.

[12] Roberts, J. W., Chalker, P. R., Ding, B., Oliver, R. A., Gibbon, J. T., Jones, L. A. H., ... & Massabuau, F. P. (2019). Low temperature growth and optical properties of  $\alpha$ -Ga<sub>2</sub>O<sub>3</sub>

deposited on sapphire by plasma enhanced atomic layer deposition. *Journal of Crystal Growth*, 528, 125254.

[13] Li, L., Wei, W., & Behrens, M. (2012). Synthesis and characterization of  $\alpha$ -,  $\beta$ -, and  $\gamma$ -Ga<sub>2</sub>O<sub>3</sub> prepared from aqueous solutions by controlled precipitation. *Solid state sciences*, 14(7), 971-981.

[14] Bravais Unit Cell Available from:

[https://www.researchgate.net/figure/Bravais-unit-cells-of-seven-lattice-systems\\_fig1\\_337551015](https://www.researchgate.net/figure/Bravais-unit-cells-of-seven-lattice-systems_fig1_337551015) [cited December 23, 2022].

[15] Sukapat, S. B. (2018). *Gallium oxide thin films for optoelectronic applications* (Doctoral dissertation, Youngstown State University).

[16] Michl, G. Generierung and Visualisierung von Kristallstrukturen.

[17] Kumar, N; Singh, D; Kumar, P.; Gangwar, J. Crystallographic Representation of polymorphs ZrO<sub>2</sub> using VESTA software. AIP Conference proceedings, volume 2142(1), pg. 0011331 - 0011336 (2019).

[18] Crystallography & Types of Crystals. Available from: <https://schoolworkhelper.net/crystallography-types-of-crystals/> [cited December 23, 2022].

[19] Yamin, M.; Islam, M.; Farooq, M. Physics Subjective. Physics of Solids, New Revised Edition (2017-2018), Muhammad Shahid Qureshi and Scholar Publications Urdu bazar Lahore, pages (1-437), 2008.

[20] Poncé, S., & Giustino, F. (2020). Structural, electronic, elastic, power, and transport properties of  $\beta$ -Ga<sub>2</sub>O<sub>3</sub> from first principles. *Physical Review Research*, 2(3), 033102.

[21] Powder X-ray Diffraction. Available from: [https://chem.libretexts.org/Bookshelves/Analytical\\_Chemistry/Supplemental\\_Modules\\_\(Analytical\\_Chemistry\)](https://chem.libretexts.org/Bookshelves/Analytical_Chemistry/Supplemental_Modules_(Analytical_Chemistry)) [cited February 22, 2022].

[22] X-ray Powder Diffraction (XRD) Available from: <https://serc.carleton.edu/researcheducation/ /techniques/XRD.html> [cited February 22, 2023].

[23] Principles of X-ray crystallography Available from: <https://www.azom.com/article.aspx?ArticleID=18684> [cited February 22, 2023].

[24] X-ray diffraction analysis. Available from:

<https://www.twi-global.com/technical-knowledge/faqs/x-ray/> [cited February 30,2023].

[25] Introduction of VESTA Available from:

<https://www.kent.ac.uk/software/vesta> [cited April 12, 2023].

[26] VESTA Manual Available from:

[https://www.xray.cz/kryst/Vesta\\_manual.pdf](https://www.xray.cz/kryst/Vesta_manual.pdf) [cited April 12, 2023].

[27] Features of Vesta Available from:

<https://jp-minerals.org/vesta/en/doc.html> [cited April 12, 2023].

[28] Zirconium Wikipedia Available from:

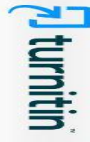
<https://en.wikipedia.org/wiki/Zirconium> [cited April 1, 2023].

[29] Crystallography. Available from:

<https://www.britannica.com/science/crystallography> [cited January 13, 2023].

[30] Jamwal, N. S., & Kiani, A. (2022). Gallium oxide nanostructures: A review of synthesis, properties and applications. *Nanomaterials*, 12(12), 2061.

[31] Stepanov, S., Nikolaev, V., Bougrov, V., & Romanov, A. (2016). Gallium OXIDE: Properties and application 498 a review. *Rev. Adv. Mater. Sci*, 44, 63-86.



Assignments

Students

Grade Book

Libraries

Calendar

Discussion

Preferences

NOV VIEWING HOME > PHYSICS > SECOND CHANCE JUNE DEFENSE 2023

### About this page

This is your assignment index. To view a paper, select the paper's title. To view a Similarity Report, select the paper's Similarity Report icon in the similarity column. A question icon indicates that the Similarity Report has not yet been generated.

## Second Chance June Defense 2023

INDEX | NOV VIEWING NEW PAPERS ▼

Submit File		Online Grading Report   Edit assignment settings   Email non-submitters						
<input type="checkbox"/>	AUTHOR	TITLE	SIMILARITY	GRADE	RESPONSE	FILE	PAPER ID	DATE
<input type="checkbox"/>	Fizza Akhbar	BS: June Defense 2023	14%				2023559190	15-May-2023